Cold-Crystallization of Poly(trimethylene terephthalate) Studied by Photoluminescence of Its Amorphous Portion

Wei-ang Luo,[†] Zhengfu Liao,[‡] Jin Yan,[†] Yunbo Li,[†] Xudong Chen,*[,†] Kancheng Mai,[†] and Mingqiu Zhang*[,†]

Key Laboratory of the Ministry of Education for Polymer Composite and Functional Materials, OFCM Institute, School of Chemistry and Chemical Engineering, Sun Yat-sen University, Guangzhou 510275, China, and Faculty of Materials and Energy, Guangdong University of Technology, Guangzhou 510006, China

Received May 20, 2008; Revised Manuscript Received July 25, 2008

ABSTRACT: Dynamic processes of isothermally cold-crystallized poly(trimethylene terephthalate) (PTT) was investigated by fluorescence spectroscopy of its amorphous region. The key issue lay in the fact that the emission at 390 nm originating from the main chain phenylene ring in the amorphous phase was correlated to the cold-crystallization. A reduction in this emission peak intensity corresponded to a gradual transition of the phenylene ring in the amorphous to crystal region. Accordingly, molecular chain movement and structure evolution of PTT in the course of cold-crystallization were carefully revealed. The experimental results indicated that the kinetics parameters measured by the fluorescence spectroscopy method are in good agreement with those by differential scanning calorimetry (DSC). What is more, the former was capable of providing detailed information about structural variations during cold-crystallization, for example, molecule arrangement in induction phase.

Introduction

Poly(trimethylene terephthalate) (PTT) is an important aromatic polyester. Its excellent resilience and processing properties make it a promising candidate in both fiber and thermoplastic engineering applications.[1−4] Furthermore, PTT has high birefringence and luminous transmittance, which are expected to be used in the fields of optical communications, optical data processing, directional couplers, and nonlinear optics.[5,6] As a semicrystalline polymer, the macroscopic properties of PTT have close relations with its microstructure and specific morphologies, such as degree of crystallization and development of the spherulites. So far, structural formation under various crystallization conditions[7−11] and melt-crystallization kinetics[12,13] of PTT have been widely studied. Very recently, we reported a thorough study on the effect of molecular weight on crystallization, melting and morphology of PTT.[14] Nevertheless, investigation of PTT's cold-crystallization kinetics is much less common, and changes in its structure and properties during cold-crystallization have remained a subject of speculation and controversy.[10] Because of its extensively potential applications, deep understanding of structure−property relationships of PTT is of both theoretical and practical importance.

To the authors' knowledge, several techniques are available for studying cold-crystallization of polymers, like simultaneous small and wide angle X-ray scattering (WAXS and SAXS) and dielectric spectroscopy (DS),[15] infrared spectroscopy (IR),[16] atomic force microscopy (AFM),[17,18] differential scanning calorimetry (DSC),[19,20] scanning electron microscopy (SEM),[21] etc. It is worth noting that, however, these methods have some shortcomings when cold-crystallization is concerned. For example, simultaneous WAXS, SAXS and DS are not easy of access. AFM and SEM are only confined to observe the morphology. DSC is not sensitive enough to demonstrate the insignificant variations in materials. In this context, a simple but sensitive technique is required.

Owing to the merits of high sensitivity and nondestructive measurements, photoluminescence (PL) is a powerful and effective tool for studying physical and chemical behaviors of macromolecules. It has received significant attention from both fundamental and practical points of view.[15−23] For example, fluorescence spectrum was used in studying intramolecular energy transfer,[22] hydration properties, efflorescence and structural heterogeneity of aqueous droplets,[23] crystallization kinetics[24,25] and relaxation process of polymer chains,[26−32] phase separation,[33,34] etc.

Like poly(ethylene terephthalate) (PET) and poly(butylene terephthalate) (PBT), PTT gives strong photoluminescence as a result of their aromatic backbone containing a phenyl ring with adjacent planar carbonyl units (see Figure 1). Since the ring is incorporated into the molecules via the chain backbone, fluorescence from the ring (i.e., intrinsic fluorescence) is able to provide more accurate information about molecular motion and microstructure of the polymer at molecular level, as compared to that from small molecule probes. In addition, the problem of probe distribution can be avoided by using the intrinsic fluorescence. It is known that PET fluorescence consists of two fluorescent components: one peak of ∼330 nm coming out of the main-chain phenylene groups in the crystalline region and the other at longer wavelengths (∼380 nm) from the phenylene in the amorphous portion.[25,35] For PBT, the main-chain phenylene fluorescence near 320 nm and that near 365 nm are assigned to monomer fluorescence mainly originating from crystalline phase and excimer fluorescence from amorphous region, respectively.[36] In the case of PTT, its intrinsic fluorescence shows one trap emission peak, whose intensity decreases with increasing temperature due to a gradual transition

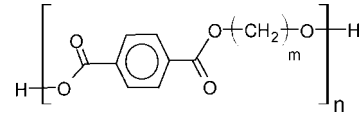

Figure 1. Schematic diagram of PET ($m = 2$), PTT ($m = 3$) and PBT ($m = 4$).

* Corresponding authors. E-mail: cescxd@mail.sysu.edu.cn (X.C.); ceszmq@mail.sysu.edu.cn (M.Z.). Phone and fax: +86-20-84113498. Key Laboratory for Polymeric Composite and Functional Materials of Ministry of Education.
[†] Sun Yat-sen University.
[‡] Guangdong University of Technology.

10.1021/ma801119n CCC: $40.75
Published on Web 09/26/2008

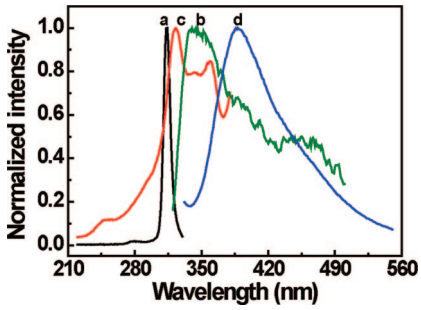

Figure 2. (a) Normalized excitation spectrum ($\lambda_{em} = 340$ nm) and (b) emission spectrum ($\lambda_{ex} = 314$ nm) of PTT solution ($c = 0.291$ mol/L); (c) normalized excitation spectrum ($\lambda_{em} = 390$ nm) and (d) emission spectrum ($\lambda_{ex} = 322$ nm) of amorphous PTT film.

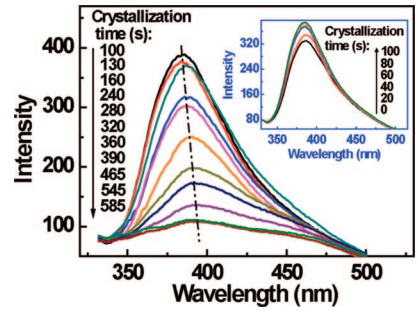

Figure 3. Fluorescence spectra of amorphous PTT film crystallizing at 60 °C for different times using a 322 nm excitation. The inset shows fluorescence spectra in the induction phase.

of the main-chain phenylene rings in amorphous form to crystalline. The photoluminescence (PL) method proved to be capable of monitoring molecular relaxations (including γ-, β- and α-transitions) and cold-crystallization dynamic process of PTT solid.[37]

Accordingly, the objectives of the present work are to expand upon fluorescence spectroscopy application in determining the dynamic process of PTT cold-crystallization during isothermal heat treatment, and to develop a direct, nondestructive and rapid technique to detect in situ change in crystallinity of the polymer. In the meantime, the motion of molecular chains and the generation and growth mechanism of PTT crystal are studied by characterizing fluorescence emission of the amorphous region.

Experimental Section

Poly(trimethylene terephthalate) (PTT) pellets, with an intrinsic viscosity of 0.91 dL/g (measured in 60/40 phenol/tetrachloroethane at 298 K) and melting point 225 °C, were provided by Shell Chemicals Co. Prior to the experiments, they were dried for 48 h under vacuum at 80 °C. A glassy amorphous film (about 30 μm thick) was prepared by pressing the pellets at 280 °C for 5 min and then quenching the sample in a liquid nitrogen bath.

Fluorescence emission spectra were collected by a RF-5301PC spectrofluorophotometer with a 150 W xenon lamp. Filmy samples were set at 45° to the exciting beam.[25] Excitation wavelength was set to 322 nm, while the slit widths were 5 nm for both excitation and emission monochromators. Temperature dependent measurements were carried out using a program controlled closed cycle liquid helium cryostat (ARS 8200). During the entire experiment, the temperature can be maintained with an accuracy of ±0.1 °C. All spectra were repeatedly recorded for 3 times to ensure perfect duplication.

Differential scanning calorimetry (DSC) measurements were performed on a Perkin-Elmer DSC-7 under nitrogen atmosphere. The instrument was calibrated with high purity melting standard indium and zinc.

Wide-angle X-ray diffraction data (WAXD) were taken on a Bruker D8 Advance Diffractometer (Germany).

Results and Discussion

1. PL Behavior of PTT Film during Cold-Crystallization. As mentioned above, PTT has fluorescent phenylene moieties in the main chain, which has fluorescence peak at 328−350 nm in chloroform−trifluoroacetic acid (4:1 v/v) mixed solvents,[37] originating from the monomeric emission commonly.[37,38] For amorphous PTT film, a single peak at around 390 nm is observed on the emission spectrum at room temperature (Figure 2). According to the PL behavior of PTT solutions and previous reports about PET and PBT film, which have similar structures as PTT, the luminescence peak of amorphous PTT film results from a ground-state dimer[38−41] or an excimeric emission.[42,43] Generally, an excimer is formed between an electronically excited chromophore and another chromophore of the same kind in the ground state, yielding a wholly overlapping sandwich structure of aromatic rings. A ground-state dimer is formed through the interaction between the same chromophores in their ground states.[44] For PTT, the dimers are stable states formed by the interaction among the phenylene moieties.[35,44] The emission at around 390 nm is ascribed to dimer fluorescence of PTT based on the following two reasons. First, the excitation spectra of monomers and excimers are the same,[45] whereas those of monomer and ground-state dimer are different.[46] Based on the resemblance between the disordered nature of macromolecular chains of PTT in solution and that in amorphous phase of a film, we have measured the excitation spectrum of PTT monomer ($\lambda_{em} = 340$ nm) in solution and that of an amorphous PTT film at $\lambda_{em} = 390$ nm (Figure 2). The results indicate that the excitation peak of monomer centers at 314 nm, while the position of excitation peak of amorphous PTT shifts to 322 nm. Thus, the emission band at 390 nm should result from dimer emission. Second, as shown by the fluorescence spectra of the amorphous PTT film crystallizing at 60 °C (Figure 3), the emission peaks at around 390 nm gradually shift to longer wavelength with increasing time. If they were produced by excimers, the peak position should be constant.[35] Therefore, the red-shift of the 390 nm peak attributes to the formation of ground-state dimers.

Interestingly, the dimers come from the phenylene in the amorphous region of PTT. This is because the π-electrons of the phenylene groups are isolated from each other in the crystalline region, but some phenylene moieties in the amorphous region can be within a distance of 0.35 nm from a phenylene or carbonyl group. Thus the π-electrons of phenylene groups would overlap and interact with the π-electrons of other phenylene groups.[25,37] In this context, it is known that the fluorescence at 390 nm represents the emission from the phenylene groups in the amorphous region of PTT. The higher the amount of crystals, the weaker the emission. Thus, the fluorescence intensity of 390 nm emission can be an indication of the crystallinity of PTT films. In this paper, the relative intensity of 390 nm has been used to discuss the correlation between cold-crystallization and the photoluminescence of PTT solid. Here, the relative intensity can be defined as

$$R = I_t/I_0 \quad (1)$$

where I_0 and I_t are fluorescence intensities at 390 nm for PTT sample crystallized at time 0 and t, respectively. Moreover, the slight fluorescence difference induced by the differentiae of films (such as different thickness of films) can be neglected by using the relative fluorescence intensity. I_t/I_0, of the samples with the same crystallinity are identical, regardless of the ways of the crystal formation. This guarantees the determination of crystallinity using the proposed photoluminescence method. Further-

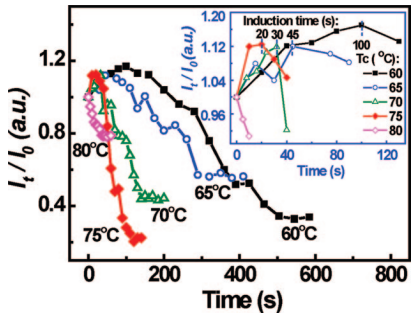

Figure 4. Dependence of fluorescence relative intensity (I_t/I_0) on crystallization time at different crystallization temperatures. The inset shows the amplified plots within the induction phase. (I_0, I_t are fluorescence intensities at 390 nm for PTT sample crystallizing at time 0 and t, respectively).

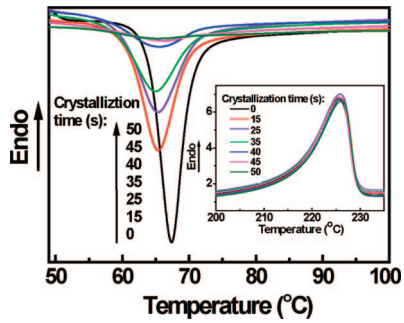

Figure 5. DSC cold-crystallization thermograms for amorphous PTT crystallizing for different time at 80 °C (inset is the DSC cold-crystallization and melting thermogram for amorphous PTT).

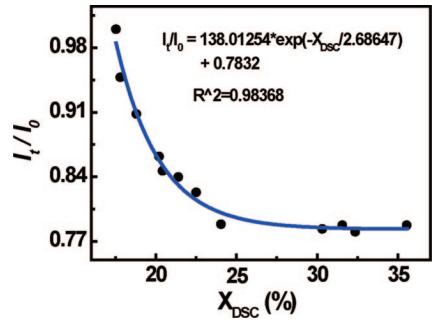

Figure 6. Relationship between fluorescence relative intensity and the crystallinity of PTT films based on DSC method at 80 °C. Both fluorescence spectroscopy and DSC methods are measured under the same conditions.

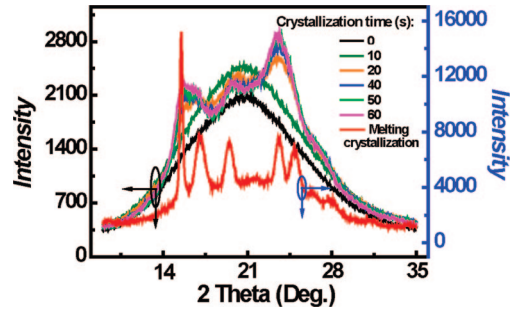

Figure 7. WAXD spectra of PTT film crystallizing under the same conditions as the change of fluorescence measured at 80 °C. The line with the right coordinate is the spectrum of PTT sample crystallized at 195 °C from the melt.

more, this treatment does not affect the calculation of kinetics latter.

Figure 4 displays the time dependences of relative intensity at different crystallization temperatures. The rising and descending parts are related to crystallization induction (see inset in Figure 4) and crystallization processes, respectively. Detailed analysis of the molecular mechanisms involved is given in the section Structure Evolution during Cold-Crystallization.

2. Correlation between Fluorescence, Crystallinity, and Crystal Form during Cold-Crystallization. For polymeric materials, WAXD and DSC are quite popular methods to measure crystallinity, and the determination of crystal structure is usually carried out by the WAXD method.[47]

Figure 5 shows the DSC cold-crystallization thermograms for amorphous PTT crystallizing at 80 °C under the same conditions as the fluorescence test. The area of the exothermal peak decreased as crystallization time increased. However, the endothermal melting peaks do not change obviously (see inset in Figure 5).

To a low crystallinity polymer, if a cold-crystallization peak appears in the heating DSC curve, its crystallinity can be obtained according to the following equation:[48]

$$X_{DSC} = (\Delta H_m - \Delta H_c)/\Delta H_0 \times 100\% \quad (2)$$

where ΔH_m is melt enthalpy of sample, ΔH_0 is the melt enthalpy of 100% PTT crystalline sample, which is 30 ± 2 kJ/mol,[49] and ΔH_c is the enthalpy of the cold-crystallization.

Figure 6 depictes the quantitative relation between the fluorescence intensity and the actual crystallinity of PTT films measured by DSC at 80 °C, which indicates that the fluorescence intensity decreases with increasing crystallinity. The correlation between the fluorescence and the actual crystallinity (X_{DSC}) is a first order exponential decay relation when PTT crystallizes at 80 °C. However, when the crystallization temperature is below 80 °C, the correlation of $I_t/I_0 \sim X_{DSC}$ becomes more complicated due to the existence of an induction period, which has not been discussed in the following section.

Figure 7 shows the WAXD spectra of PTT film crystallizing at 80 °C, under the same conditions where the change of fluorescence is measured. Obviously, each sample exhibits seven characteristic peaks at the diffractional angles 2θ of 15.3, 16.8, 19.4, 21.8, 23.6, 24.6, and 27.3°, corresponding to the reflection planes of (010), (0$\bar{1}$2), (012), (10$\bar{2}$), (102), (1$\bar{1}$3) and (10$\bar{4}$), respectively.[50] Because of the low crystallininty and imperfection of cold-crystallized PTT, the peaks at 19.4° and 24.6° are not very clear. It is also apparent from Figure 7 that crystallization of PTT for different crystallization times (at least within the range studied) does not affect the positions of these characteristic peaks, indicating that the crystal form of PTT does not change with varying crystallization time. According to prior report,[51] it has been determined that the crystal unit cell of PTT (based on WAXD results) is triclinic with axes a = 4.64 Å, b = 6.27 Å and c = 18.64 Å, and angles α = 98°, β = 90°, and γ = 112°, with an antichiral packing of molecules only along the c-axis. The space group proposed for this crystal modification is P$\bar{1}$.[51] Moreover, Figure 7 shows that no obvious crystal diffractional peaks are seen when the crystallization time is shorter than 20 s. The crystallinity calculated by WAXD is 26.87%, 37.25%, 39.06%, and 40.32% at crystallization time 20, 40, 50 and 60 s, respectively. This phenomenon indicates that the fluorescence intensity decreases with increasing crystallinity. On the basis of intensity-dependence of the emission at 390 nm on crystallinity, the fluorescence spectrum can be used to monitor the dynamic process of cold-crystallization of PTT.

3. Analysis of Isothermal Cold-Crystallization Kinetics. The discussion in the section PL Behavior of PTT Film during Cold-Crystallization demonstrates that the cold-crystallization of PTT is closely related to the fluorescence behavior at around

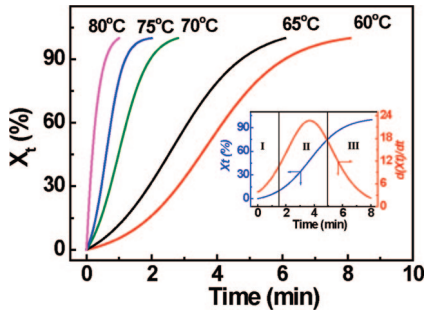

Figure 8. Dependence of relative crystallinity on crystallization time of cold-crystallized PTT at different temperatures obtained by fluorescence spectrum method. The inset shows $X_t \sim t$ plot and its differential curve at 60 °C, which can be divided into three phases: (I) nucleation phase; (II) nucleus growth phase; and (III) secondary crystallization phase.

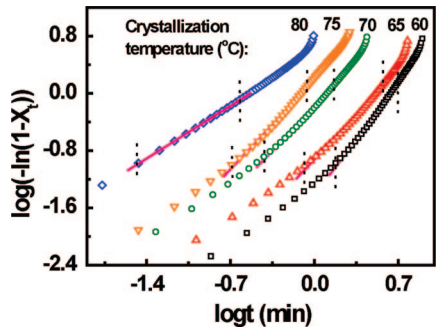

Figure 9. Avrami plots of isothermally cold-crystallized PTT measured by the fluorescence method.

390 nm of its amorphous region. Naturally, the relative crystallinity of PTT during the cold-crystallization process can be estimated from[25]

$$X_t = (R_t - R_0)/(R_\infty - R_0) \quad (3)$$

where X_t is relative crystallinity at time t; R_t and R_0 are fluorescence relative intensities at time t and at the beginning, respectively; R_∞ is the minimum relative intensity during the crystallization. By using eq 3 and the experimental data in Figure 4, we obtain the time dependences of crystallinity of cold-crystallized PTT (Figure 8).

The most common approach for describing isothermal crystallization kinetics is the Avrami model,[12] in which the relative crystallinity as a function of time is expressed as follows:

$$\log[-\ln(1 - X_t)] = \log K + n \log t \quad (4)$$

where K and n stand for rate constant and the Avrami exponent, respectively. Both K and n depend on nucleation and growth mechanisms of spherulites, and can be obtained from the linear regression curve of $\log[-\ln(1 - X_t)] \sim \log t$.

Figure 9 shows the Avrami plots of amorphous PTT isothermally cold-crystallized at different temperatures measured by the fluorescence spectrum method. It is seen that the plots also distinguish primary crystallization from secondary crystallization. That is, crystallization at linear stage represents primary crystallization, while secondary crystallization occurs at nonlinear stage. Primary crystallization consists of outward growth of lamellar stacks until impingement, and secondary crystallization, which may well overlap with primary crystallization, is filling in the spherulites of interstices.[52] As we focus only on the kinetics of primary crystallization, the best-fit lines were drawn except the initial points in the nucleation regime and the secondary crystallization (the points deviating from the linearity at the end of crystallization). Nevertheless, the distinct three parts revealed by the Avrami plots enable us to identify the corresponding phases on the $X_t \sim t$ plot (see the inset of Figure 8).

Table 1. Avrami Crystallization Kinetics Parameters of Cold-Crystallized Amorphous PTT Determined by Fluorescence Spectrum and DSC Methods

	fluorescence spectrum method				DSC method			
T (°C)	n	K (min^{-n})	$t_{1/2}$ (min)	ΔE (kJ/mol)	n	K (min^{-n})	$t_{1/2}$ (min)	ΔE (kJ/mol)
60	2.21	0.038	3.72		2.38	0.011	5.70	
65	1.78	0.120	2.68		2.36	0.035	3.54	
70	1.74	0.637	1.05	228.0	1.61	0.273	1.78	237.5
75	1.76	1.498	0.65		1.53	0.564	1.14	
80	1.05	3.652	0.21		1.97	1.217	0.75	

Returning to the study of cold-crystallization kinetics, Table 1 lists the kinetic parameters (incl. the aforesaid K and n, activation energy, ΔE, and half-time of crystallization, $t_{1/2}$), in comparison with those determined by the DSC method. Evidently, the exponent n for the primary crystallization measured by fluorescence spectrum method ranges from 1.05 to 2.21, which suggests a two-dimensional crystal development for the cold-crystallized PTT film, representing outward growth of lamellar stacks prior to impingement. The nonintegral n value may also be considered due to crystal branching and/or two-stage crystal growth and/or mixed growth and nucleation mechanisms.[53] After primary crystallization, the crystalline clusters grow rapidly, which will eventually be linked into three-dimensional networks, resulting in the formation of sheaflike or rodlike structures.[11] The size of sheaflike or rodlike crystallite is relatively small, so that the crystal superstructure is difficult to be resolved by polarized light microscope. This is evidenced by the wide-angle X-ray diffraction patterns in Figure 7. The cold-crystallized PTT shows much wider crystalline peaks than melt-crystallized PTT that is characterized by spherulitic morphology.[14] As X-ray data serve as a semiquantitative link between crystallinity and crystal perfection,[54] it is understood that cold-crystallized PTT possesses reduced internal order and/or size of crystals as compared to its melt-crystallized version.

Table 1 also shows that the rate constant K and $t_{1/2}$ ($t_{1/2} = (\ln 2/K)^{1/n}$) of cold-crystallization of PTT are very sensitive to crystallization temperature. They increase with increasing temperature, following the Arrhenius relation. In general, the crystallization rate of a polymer is controlled by nucleation and diffusion mechanisms.[53] For cold-crystallization, viscously driven diffusion process plays the leading role,[53] resulting in rapid variation in the rate of cold-crystallization with temperature. On the other hand, the crystallization activation energy is estimated at 228 kJ/mol. This high energy value implies that a lot of PTT monomer units must be reoriented during cold-crystallization.

The Avrami exponent based on the DSC method is found to be 1.53−2.38, while the activation energy is 237.5 kJ/mol, slightly greater than those obtained by the fluorescence spectrum method. The differences between these two methods should result from the fact that different test methods collect changes in different physical quantities, while the perturbation response speed of each physical quantity has its distinctness.

4. Structure Evolution during Cold-Crystallization. A careful examination of Figure 3 indicates that the fluorescence peak intensity at around 390 nm of amorphous PTT film cold-crystallized at 60 °C changes with time in different ways at different stages. With a rise in time, the peak intensity increases within 0−100 s, while it starts to decrease when the crystallization time exceeds 100 s. The phenomenon manifests that the cold-crystallization process of PTT can be divided into two

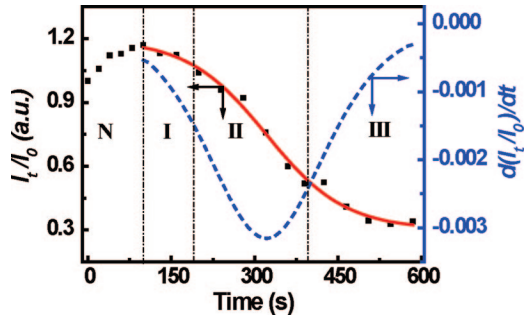

Figure 10. Dependence of fluorescence relative intensity (I_t/I_0) on crystallization time (solid line) and its differential curve (dash line). Crystallization temperature is 60 °C. The dynamic process includes four phases: (N) crystallization induction phase; (I) nucleation phase; (II) nucleus growth phase; and (III) secondary crystallization phase. (I_0, I_t are fluorescence intensities at 390 nm for PTT sample crystallizing at time 0 and t, respectively).

stages: crystallization induction stage (see the inset in Figure 3) and crystallization stage. Since the above analysis based on Figures 8 and 9 demonstrates that the crystallization stage consists of three phases, it can be concluded that the entire cold-crystallization of PTT is a four-phased process: (N) crystallization induction phase; (I) nucleation phase; (II) nucleus growth phase; and (III) secondary crystallization phase[11] (Figure 10).

In the crystallization induction phase (namely, phase N), fluorescence intensity increases with increasing heat treatment time. The enhanced emission is induced by the interaction between the parallel aromatic rings belonging to different polymer chains. A parallel arrangement of molecular chains in given regions creates a density fluctuation growing with time. Crystal nucleation occurs in denser regions of density fluctuation once the size of the fluctuation exceeds a given value. The inset in Figure 4 clearly shows that the characteristic time of the induction phase decreases with increasing crystallization temperature. The induction time ranges from 100 to 20 s when crystallization temperatures increase from 60 to 75 °C. Although the crystallization at 80 °C is so fast that the induction phase is nearly invisible, the PL method has exhibited its sensitivity superior to DSC. The latter cannot detect the induction phase even if the cold-crystallization temperature is sufficiently low.

After the induction phase, amorphous PTT undergoes crystallization, and its fluorescence intensity decreases with time (Figure 3). The reduction of fluorescence intensity is due to a gradual transfer of phenylene groups from amorphous to crystalline region, which is equivalent to an increase in crystallinity. There were opposite results reported by Clauss and Salem.[39] They suggested that the increase in fluorescence intensity of PET films at higher orientations arose from scattering between crystallites, but they also pointed out that the level of crystalline order is insufficient to produce light scattering in the low crystalline region. The light scattering does not affect the emission intensity due to the low crystallinity in our case. A careful survey of phase I (Figure 10) indicates that the fluorescence intensity decreases slowly at the early stage of crystallization. This means that the adjacent molecular chains are being oriented in parallel with each other to form a large amount of tiny crystallites (sheaflike crystals). Meanwhile, in the crystallites, the interplanar spacing of two nearest phenylene rings increases, and π-electrons of the phenylene groups are isolated from each other. This regime is thus named the nucleation phase.

In phase II, the emission decreases rapidly with increasing crystallinity. Those sheaflike crystals probably act as junction points upon which the aggregate structures grow until they impinge with each other. This process is known as the nucleus

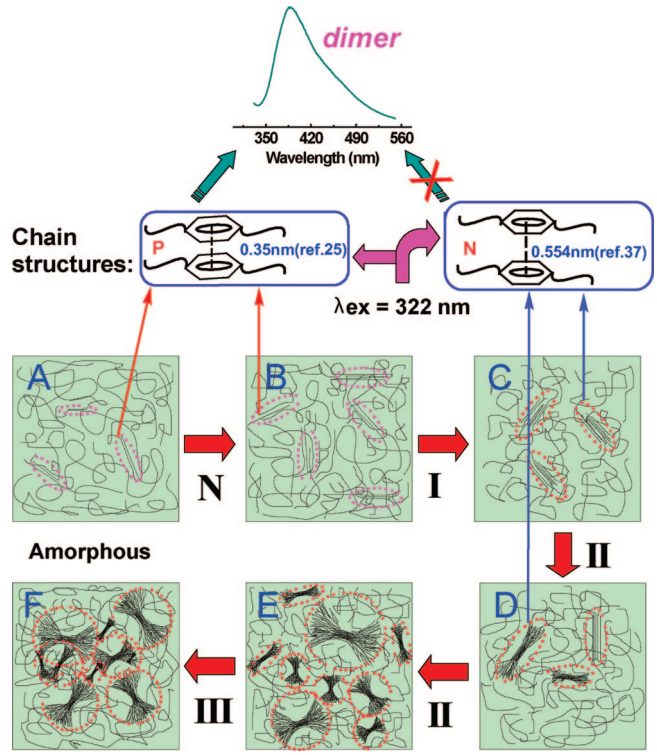

Figure 11. Movement of molecular chains and structure evolution of cold-crystallized PTT: (N) crystallization induction phase; (I) nucleation phase; (II) nucleus growth phase; and (III) secondary crystallization phase.

growth phase. Both phases I and II may be regarded as a primary crystallization. In phase III, growth of the sheaflike crystallite is impinged and subsequently interconnected network is formed. The fluorescence decreases slowly with increasing time. The phenomenon resembles secondary crystallization. As crystallization time is further increased, the aggregation or propagation of sheaflike crystallites would take place in order to reduce surface free energy, resulting in the formation of sheaflike or rodlike structures.[11]

According to the above analysis, a model is proposed to depict the entire evolvement of PTT chains during cold-crystallization (Figure 11). In amorphous PTT, there exist some structures with parallel arrangement (named as "P" structures) of the molecular chains. When these structures are excited at 322 nm, they have dimer emission at 390 nm. During the induction phase, these "P" structures get more numerous and larger, leading to an increase of dimer fluorescence. As the "P" structure grows up to a critical size to become a crystal nucleus, the molecular chains arrange to nucleation structure (named as "N" structure), while this "N" structure cannot form dimer due to the large distance among phenylene groups. Once the crystallization phase begins, the crystal portion becomes larger and larger, and the "N" structures become the majority of the molecular chain structures. Therefore, the dimer fluorescence intensity decreases with increasing cold-crystallization time.

Summary

In summary, structural formation of PTT crystallites and its kinetics during isothermal cold-crystallization were successfully investigated in terms of fluorescence spectroscopy of amorphous portion in PTT. The emission spectra of amorphous PTT films only showed an individual peak at 390 nm. Its intensity was correlated with the development of PTT crystalline structure, from parallel arrangement structure of molecular chains to sheaflike or rodlike crystal structures. The kinetics results

obtained by the fluorescence spectrum method are in good agreement with those obtained by the DSC method.

As an evaluation of performance of the fluorescence spectroscopy method, interpretability of the spectral changes taking place in the cold-crystallization process of PTT was investigated in relation to time-dependent structural evolution. It proved that the intrinsic fluorescence technique is a suitable tool for investigating the dynamic crystallization process of polymers.

The most interesting merit of the fluorescence spectrum method discussed in this work lay in its sensitiveness in structural characterization, which made the observed spectral variability more intuitive and comprehensible. The method gave appropriate information for understanding and interpreting the structural changes of PTT during cold-crystallization, especially the details of the induction phase. In contrast, the DSC method only provided the information about enthalpy changes, and failed to illuminate the motion of molecular chains and structure evolution at a molecular level like the fluorescence spectrum method.

According to the working principle revealed in this work, the fluorescence spectroscopy method should be capable of studying not only cold-crystallization but also other crystallization processes (like melt crystallization, solvent induced crystallization, etc.) of crystallizable polymers, so long as their molecules contain chromophores. Further works in this aspect are being carried out in the authors' laboratory.

Acknowledgment. X.C. acknowledges the financial support from the program of National Natural Science Foundation of China (Grant No. 50673104) and Natural Science Foundation of Guangdong province (Grant No. 7003702).

References and Notes

(1) Kim, K. J.; Bae, J. H.; Kim, Y. H. *Polymer* **2001**, *42*, 1023.
(2) Wu, G.; Li, H. W.; Wu, Y. Q.; Cuculo, J. A. *Polymer* **2002**, *43*, 4915.
(3) Chang, J. H.; Kim, S. J.; Im, S. *Polymer* **2004**, *45*, 5171.
(4) Brown, H. S.; Chuah, H. H. *Chem. Fibers Int.* **1997**, *47*, 72.
(5) Singh, G. K.; Low, A. L. Y.; Yong, Y. S. *Optik* **2004**, *115*, 334.
(6) Bai, S. J.; Spry, R. J.; Jr, M. D. A.; Barkley, J. R. *J. Appl. Phys.* **1996**, *79*, 9326.
(7) Shafee, E. E. *Polymer* **2003**, *44*, 3727.
(8) Hong, P. D.; Chuang, W. T.; Yeh, W. J.; Lin, T. L. *Polymer* **2002**, *43*, 6879.
(9) Wang, Y.; Shen, D. Y.; Qian, R. Y. *J. Polym. Sci., Polym. Phys. Ed.* **1998**, *36*, 783.
(10) Cho, J. W.; Woo, K. S. *J. Polym. Sci., Part B: Polym. Phys.* **2001**, *39*, 1920.
(11) Chuang, W. T.; Hong, P. D.; Shih, K. S. *Polymer* **2004**, *45*, 8583.
(12) Xu, Y.; Jia, H. B.; Ye, S. R.; Qian, J. W. *J. Mater. Sci. Lett.* **2006**, *41*, 8390.
(13) Huang, J. M.; Chang, F. C. *J. Polym. Sci., Part B: Polym. Phys.* **2000**, *38*, 934.
(14) Chen, X. D.; Hou, G.; Chen, Y. J.; Yang, K.; Dong, Y. P.; Zhou, H. *Polym. Test.* **2007**, *26*, 144.
(15) Šics, I.; Ezquerra, T. A.; Nogales, A.; Denchev, Z.; Alvarez, C.; Funari, S. S. *Polymer* **2003**, *44*, 1045.
(16) Yoshii, T.; Yoshida, H.; Kawai, T. *Thermochim. Acta* **2005**, *431*, 177.
(17) Ivanov, D. A.; Amalou, Z.; Magonov, S. N. *Macromolecules* **2001**, *34*, 8944.
(18) Ivanov, D. A.; Pop, T.; Yoon, D. Y.; Jonas, A. M. *Macromolecules* **2002**, *35*, 9813.
(19) Supaphol, P.; Spruiell, J. E. *Polymer* **2001**, *42*, 699.
(20) Ziaee, Z.; Supaphol, P. *Polym. Test.* **2006**, *25*, 807.
(21) Sun, Y. S.; Woo, E. M. *Polymer* **2001**, *42*, 2241.
(22) Gatica, N.; Marcelo, G.; Mendicuti, F. *Polymer* **2006**, *47*, 7397.
(23) Choi, M. Y.; Chan, C. K.; Zhang, Y. H. *J. Phys.Chem. A* **2004**, *108*, 1133.
(24) Schonherr, H.; Frank, C. W. *Macromolecules* **2003**, *36*, 1188.
(25) Itagaki, H.; Kato, S. *Polymer* **1999**, *40*, 3501.
(26) Martins, T. D.; Gulmine, J. V.; Akcelrud, L.; Weiss, R. G.; Atvars, T. D. Z. *Polymer* **2006**, *47*, 7414.
(27) van den Berg, O.; Sengers, W. G. F.; Jager, W. F.; Picken, S. J.; Wübbenhorst, M. *Macromolecules* **2004**, *37*, 2460.
(28) Dibbern-Brunelli, D.; Atvars, T. D. Z. *J. Appl. Polym. Sci.* **2000**, *75*, 815.
(29) Martins-Franchetti, S. M.; Atvars, T. D. Z. *Eur. Polym. J.* **1995**, *31*, 459.
(30) Christoff, M.; Atvars, T. D. Z. *Macromolecules* **1999**, *32*, 6093.
(31) Vigil, M. R.; Bravo, J.; Atvars, T. D. Z.; Baselga, J. *Macromolecules* **1997**, *30*, 4871.
(32) Corrales, T.; Peinado, C.; Bosch, P.; Catalina, F. *Polymer* **2004**, *45*, 1545.
(33) Horinaka, J.; Matsumura, Y.; Yamamoto, M.; Aoshima, S.; Kobayashi, E. *Polym. Bull.* **1999**, *42*, 85.
(34) Crenshaw, B. R.; Weder, C. *Adv. Mater.* **2005**, *17*, 1471.
(35) Itagaki, H.; Inagaki, Y.; Kobayashi, N. *Polymer* **1996**, *37*, 3553.
(36) Itagaki, H.; Arakawa, S. *Polymer* **2003**, *44*, 3921.
(37) Luo, W. A.; Chen, Y. J.; Chen, X. D.; Liao, Z. F.; Mai, K. C.; Zhang, M. Q. *Macromolecules* **2008**, *41*, 3912.
(38) Hemker, D. J.; Frank, C. W. *Polymer* **1988**, *29*, 437.
(39) Clauss, B.; Salem, D. R. *Polymer* **1992**, *33*, 3193.
(40) Hennecke, M.; Kurz, K.; Fuhrman, J. *Colloid Polym. Sci.* **1987**, *265*, 674.
(41) Hashimoto, H.; Hasegawa, M.; Horie, K.; Yamashita, T.; Ushiki, H.; Mita, I. *J. Polym. Sci., Part B: Polym. Phys.* **1993**, *31*, 1187.
(42) Qian, R. Y.; Bai, F. L.; Chen, S. X. *Chin. Sci. Bull.* **1982**, *27*, 725.
(43) Cao, T.; Magonov, S. N.; Qian, R. Y. *Polym. Comm.* **1988**, *29*, 43.
(44) Itagaki, H.; Horie, K.; Mtta, I. *Prog. Polym. Sci.* **1990**, *15*, 361.
(45) Allen, N. S.; Mckellar, J. F. *Makromol. Chem.* **1978**, *179*, 523.
(46) Teyssèdre, G.; Menegotto, J.; Laurent, C. *Polymer* **2001**, *42*, 8207.
(47) Martínez-Palau, M.; Franco, L.; Puiggalí, J. *Polymer* **2007**, *48*, 6018.
(48) Chen, S. H.; Wu, Y. H.; Su, C. H.; Jeng, U.; Hsieh, C. C.; Su, A. C.; Chen, S. A. *Macromolecules* **2007**, *40*, 5353.
(49) Pyda, M.; Boller, A.; Grebowicz, J.; Chuah, H.; Lebedev, B. V.; Wunderlich, B. *J. Polym. Sci., Part B: Polym. Phys.* **1998**, *3*, 2499.
(50) Dangseeyun, N.; Srimoaon, P.; Supaphol, P.; Nithitanakul, M. *Thermochim. Acta* **2004**, *409*, 63.
(51) Wang, B. J.; Li, C.; Hanzlicek, J.; Cheng, S. Z. D.; Geil, P. H.; Grebowicz, J.; Ho, R. M. *Polymer* **2001**, *42*, 7171.
(52) Xu, Y.; Ye, S. R.; Bian, J.; Qian, J. W. *J. Mater. Sci.* **2004**, *39*, 5551.
(53) Hong, P. D.; Chung, W. T.; Hsu, C. F. *Polymer* **2002**, *43*, 3335.
(54) Androsch, R.; Wunderlich, B. *Polymer* **2005**, *46*, 12556.

MA801119N